J Therm Anal Calorim (2017) 130:2369–2387
DOI 10.1007/s10973-017-6495-x

A new method for assessment of glass transition temperature of ionic liquids from structure of their cations and anions without using any computer codes

Mohammad Hossein Keshavarz[1] · Karim Esmaeilpour[1] · Mehdi Heidari Saani[2] · Hedayatollah Taghizadeh[1]

Received: 21 November 2016 / Accepted: 22 May 2017 / Published online: 6 June 2017

Abstract This work introduces two simple correlations to assess the glass transition temperature of five different kinds of ionic liquids (ILs) including imidazolium, pyridinium, ammonium, sulfonium and triazolium without using any computer code. The first model is based only suitable combination of elemental composition of cations and anions divided by their molar masses. The second model improves the reliability of the first one by considering the contribution of some specific cations and anions. The reliability of two correlations will be compared with one the best reliable method, which is based on complex descriptors. For 139 ILs where the computed results of the representative model were available, the root mean square (rms) deviations of the first, the second and the representative models from the experimental data are 16.96, 7.60 and 9.28 K, respectively. Thus, the improved second correlation provides higher reliable results. The reliability of two correlations has also been checked for further 30 ILs where the values of the rms of the first and the second correlations are 12.50 and 9.92 K, respectively. In contrast to available methods, which are usually based on complex molecular descriptors and specific computer codes, the new method can easily calculate the glass transition temperatures of ILs including imidazolium, pyridinium, ammonium, sulfonium and triazolium.

✉ Mohammad Hossein Keshavarz
mhkeshavarz@mut-es.ac.ir; keshavarz7@gmail.com

[1] Department of Chemistry, Malek-ashtar University of Technology, Shahin-shahr, P.O. Box 83145/115, Islamic Republic of Iran

[2] Physics Group, Malek-ashtar University of Technology, Shahin-shahr, P.O. Box 83145/115, Islamic Republic of Iran

Keywords Glass transition temperature · Prediction · Ionic liquid · Ionic structure

Introduction

Ionic liquids (ILs) have melting points below 100 °C, which are composed entirely of cations and anions. They have suitable characteristics such as negligible vapor pressure, high heat capacity, high density, high thermal conductivity, high thermal stability and the existence of liquid state over a wide range of temperature. They have been used in different research fields such as lithium battery, solar cells and fuel cells [1, 2]. Some classes of ILs containing energetic cations or anions have also some applications as new energetic compounds, e.g., high explosives and propellants [3–6]. Due to importance of ILs, some new methods have been developed to predict different physical and thermodynamic properties as well as thermal stabilities, e.g., density [7–11].

The glass transition temperature of a material shows the reversible transition in amorphous materials from a hard and relatively brittle "glassy" state into a viscous or rubbery state, quite below the melting point, by increasing temperature. It is one of the most important properties of amorphous polymer [12–15]. It is one of the important properties for ILs because viscosity and conductivity are often reflected in the glass transition where low values leading to favorable properties [16]. Differential scanning calorimetry and differential thermal analysis (DSC/DTA) were usually used to determine the glass transition of ILs.

Due to the lack of experimental data for the large number kinds of ILs, it is essential to develop available mathematical models to predict the glass transition temperature of ILs. Several models have been developed for

predicting the glass transition temperature of one kind or multiple kinds of ILs using available literature data. Mirkhani et al. [17] introduced a quantitative structure–property relationship (QSPR) model to forecast glass transition temperature of 73 ammonium-based ILs. Mousavisafavi and coauthors [18] used a QSPR method to develop linear and nonlinear models for estimation of the glass transition temperature of 109 1,3-dialkyl imidazolium ILs. These QSPR models are limited to one kind of ILs. Mirkhani et al. [19] used QSPR method to estimate the glass transition temperature of 139 ILs. Yan et al. [20] developed a QSPR model on the basis of the general topological index (TI) for predicting the glass transition temperatures of five kinds of ILs including imidazolium, pyridinium, ammonium, sulfonium and triazolium. The QSPR model of Yan et al. [20] has the following form:

$$T_{g,IL} = 431.847 + \sum_{i=1}^{7} \alpha_{cat,i} \times TI_{cat,i} + \sum_{j=1}^{16} \alpha_{ani,j} \times TI_{ani,j} + \sum_{h=1}^{2} \alpha_{to,h} \times TI_{to,h} \quad (1)$$

where $T_{g,IL}$ is the glass transition temperature of a desired ionic liquid in K; $TI_{cat,i}$, $TI_{ani,j}$ and $TI_{to,h}$ are TIs generated from cation, anion and their interaction, respectively; $\alpha_{cat,i}$, $\alpha_{ani,j}$ and $\alpha_{to,h}$ are parameters, which depend on the type of TIs. Although the accuracy of these QSPR methods is high, they have three limitations: (1) they are based on complex descriptors; (2) they require special computer codes; and (3) they need the expert users. Gharagheizi et al. [21] introduced a group contribution (GC) method for the estimation of the glass transition temperature of 496 ILs. Lazzús [22] developed another GC method for predicting the glass transition temperature of 496 ILs. Mokadem and coworkers [23] introduced a group interaction contribution method for the estimation of glass transition temperature of 368 ILs. They proposed two models requiring binary interactions between single groups with three order contributions. Accuracy of group contribution methods is usually less than the QSPR methods. Moreover, GC methods can be applied only for those ILs that the contributions of cations and anions have been considered. These QSPR and GC models have the advantage that they can be used for predicting the glass transition temperature of multiple kinds of ILs.

The purpose of this work is to introduce two new correlations on the basis of the molecular structure of cations and anions for accurate and reliable prediction of the glass transition temperature of five kinds of ILs including imidazolium, pyridinium, ammonium, sulfonium and triazolium. The predicted results will be compared with the computed outputs of QSPR model of Yan et al. [20]. For some further ILs, the predicted results will be compared with the measured values.

Materials and methods

Experimental data of glass transition temperature of 139 ionic liquids are given in Table 1, which were used by Yan et al. [20] as training and test sets for developing QSPR model. They are based on five kinds of ILs, which are 63 imidazolium, 17 pyridinium, 48 ammonium, 7 sulfonium. These data were used to derive new correlations. The results have shown that the following general equation, which was obtained by the best fit to experimental data through multiple linear regression method [24], can correlate with elemental composition of cations and anions as:

$$T_{g,IL} = 322.62 + \frac{2153.5(n_C)_{cat} - 554.10(n_H)_{cat} + 2202.4(n_N)_{cat} + 1466.9(n_O)_{cat}}{\text{Molar mass}_{cat}} - \frac{2355.7(n_C)_{ani} + 3285.6(n_N)_{ani} + 3253.8(n_O)_{ani} + 4929.4(n_F)_{ani} + 7389.7(n_{Cl})_{ani} + 15242(n_{Br})_{ani} + 5257.9(n_S)_{ani}}{\text{Molar mass}_{ani}} \quad (2)$$

where $(n_C)_{cat}$, $(n_H)_{cat}$, $(n_N)_{cat}$ and $(n_O)_{cat}$ are the number of carbon, hydrogen, nitrogen and oxygen atoms in cation, respectively; $(n_C)_{ani}$, $(n_N)_{ani}$, $(n_O)_{ani}$, $(n_F)_{ani}$, $(n_{Cl})_{ani}$, $(n_{Br})_{ani}$ and $(n_S)_{ani}$ are the number of carbon, nitrogen, oxygen, fluorine, chlorine, bromine and sulfur atoms in anion, respectively; Molar mass_{cat} and Molar mass_{ani} are the molar mass (g mol^{-1}) of cation and anion, respectively. Since the contributions of the other elemental composition do not change the coefficient of determination or R-squared values of Eq. (2), their existences were neglected.

Besides the contribution of elemental composition, the existence of some specific cations or anions may enhance or reduce glass transition temperature of ionic liquids. Thus, the effects of these specific anions or cations can be considered besides those variables given in Eq. (2).

Table 1 Comparison of the predicted $T_{g,IL}/K$ and $T_{g,IL}^{corr}/K$ of ionic liquids by Eqs. (2) and (3) as well as training and test of Yan et al. [20] with the experimental data

Cation	Anion	Exp.*	Eq. (2)	Dev	Eq. (3)	Dev	Yan et al.	Dev
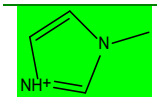	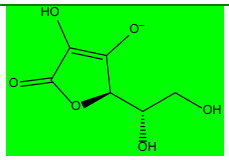	280.04	240.39	–39.65	285.39	5.35	249.69	–30.35
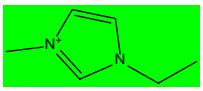	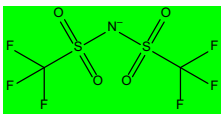	181.15	205.53	24.38	188.48	7.33	184.78	3.63
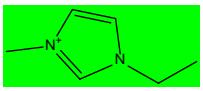	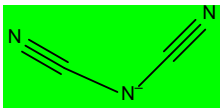	169.15	203.06	33.91	185.65	16.50	170.32	1.17
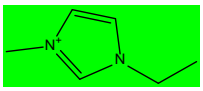	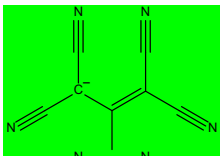	214.15	217.45	3.30	216.26	2.11	209.72	–4.43
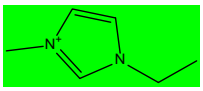		220.15	214.76	–5.39	214.07	–6.08	228.24	8.09
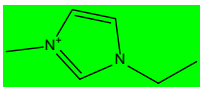	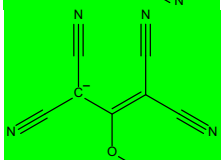	208.15	217.71	9.56	217.05	8.90	206.74	–1.41
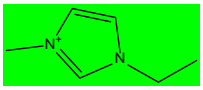	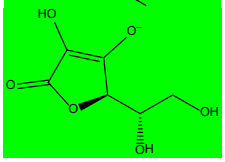	244.68	231.44	–13.24	247.93	3.25	247.61	2.93
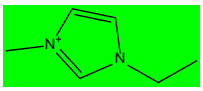	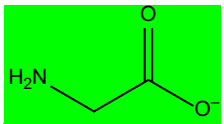	208.15	227.80	19.65	213.88	5.73	207.59	–0.56
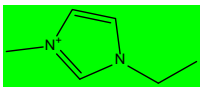		216.15	230.03	13.88	215.27	–0.88	222.70	6.55

Table 1 continued

Cation	Anion	Exp.*	Eq. (2)	Dev	Eq. (3)	Dev	Yan et al.	Dev
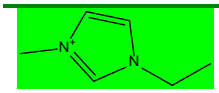	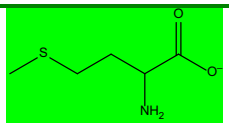	216.15	242.62	26.47	220.84	4.69	202.79	−13.36
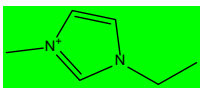	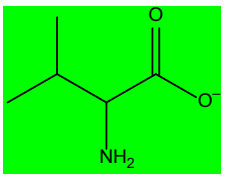	221.15	236.29	15.14	219.81	−1.34	222.65	1.50
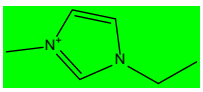	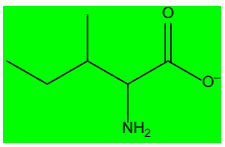	221.15	239.84	18.69	222.51	1.36	220.72	−0.43
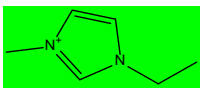	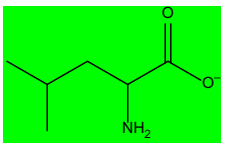	222.15	239.84	17.69	222.51	0.36	228.29	6.14
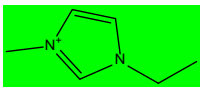	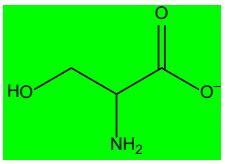	224.15	230.41	6.26	229.74	5.59	230.52	6.36
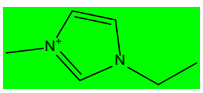	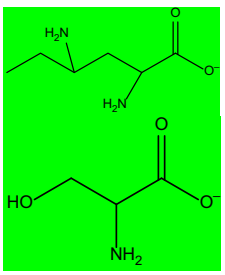	226.15	236.22	10.07	233.02	6.87	237.07	10.92
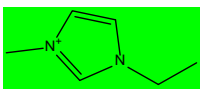		233.15	233.41	0.26	231.84	−1.31	230.66	−2.49
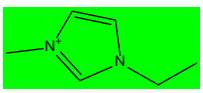	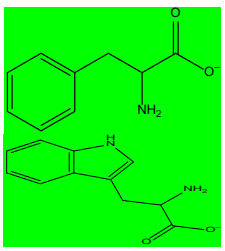	237.15	234.86	−2.29	231.63	−5.52	239.59	2.44
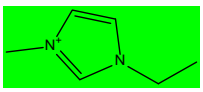		242.15	231.77	−10.38	228.89	−13.26	246.97	4.82
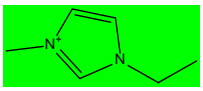	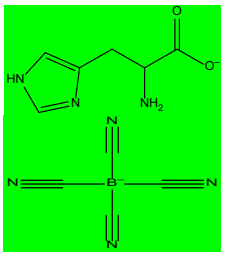	249.15	225.80	−23.35	248.56	−0.59	254.62	5.47
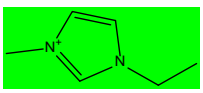		250.15	227.22	−22.93	250.99	0.84	253.26	3.11

Table 1 continued

Cation	Anion	Exp.*	Eq. (2)	Dev	Eq. (3)	Dev	Yan et al.	Dev
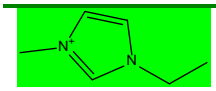	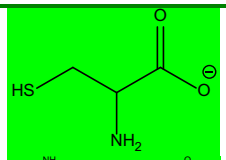	254.15	239.57	−14.58	257.92	3.77	222.34	−31.81
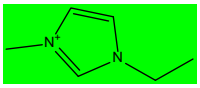	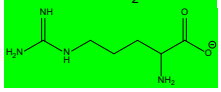	255.15	227.46	−27.69	252.25	−2.90	249.72	−5.43
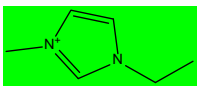	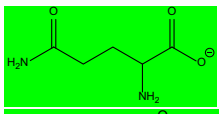	257.15	227.21	−29.94	253.12	−4.03	249.95	−7.20
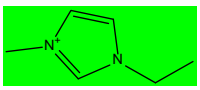	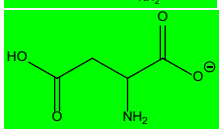	261.15	229.97	−31.18	255.14	−6.01	261.36	0.21
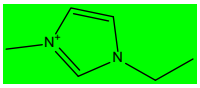	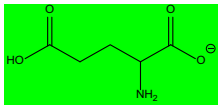	278.15	228.91	−49.24	276.91	−1.24	252.67	−25.48
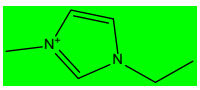	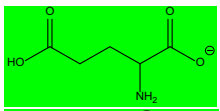	279.15	231.48	−47.67	278.72	−0.43	265.51	−13.64
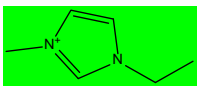	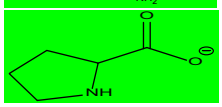	225.15	236.29	11.14	233.38	8.23	242.51	17.36
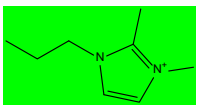	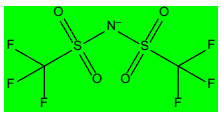	204.15	200.19	−3.96	198.43	−5.72	200.24	−3.91
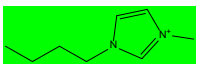	Br	223.15	227.52	4.37	226.89	3.74	226.15	3.00
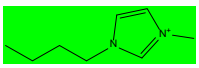	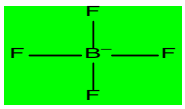	190.15	191.15	1.00	191.60	1.45	188.06	−2.09
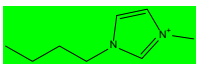	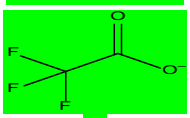	195.15	188.17	−6.98	192.43	−2.72	195.86	0.71
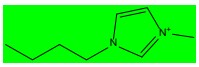	Cl	204.15	209.83	5.68	210.78	6.63	206.74	2.59
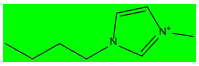	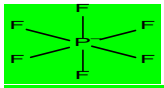	196.15	214.27	18.12	197.43	1.28	191.33	−4.82
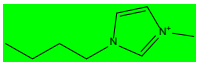	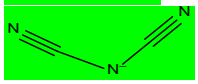	183.15	197.72	14.57	182.03	−1.12	182.59	−0.56
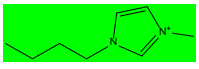	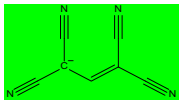	211.15	208.31	−2.84	209.53	−1.62	206.11	−5.04

Table 1 continued

Cation	Anion	Exp.*	Eq. (2)	Dev	Eq. (3)	Dev	Yan et al.	Dev
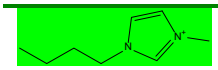	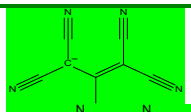	208.15	212.11	3.96	212.64	4.49	212.12	3.97
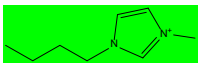	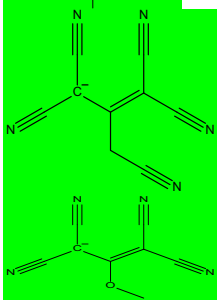	219.15	209.42	−9.73	210.44	−8.71	228.53	9.38
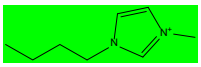		208.15	212.37	4.22	213.43	5.28	208.17	0.02
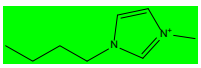	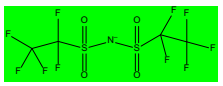	189.15	193.31	4.16	193.04	3.89	193.83	4.68
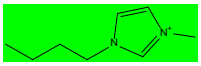	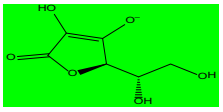	251.67	226.10	−25.57	244.31	−7.36	248.64	−3.03
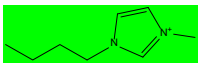	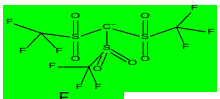	208.15	201.67	−6.48	199.52	−8.63	200.83	−7.32
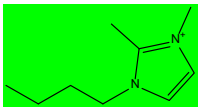	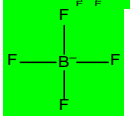	205.15	189.21	−15.94	190.28	−14.87	205.60	0.45
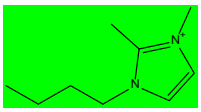	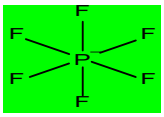	215.15	212.33	−2.82	209.69	−5.46	209.30	−5.85
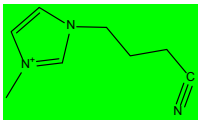	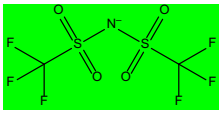	202.45	218.92	16.47	198.86	−3.59	210.06	7.61
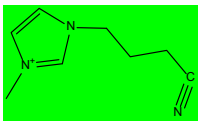	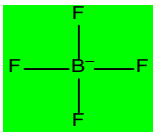	209.95	209.88	−0.07	205.60	−4.35	210.88	0.93
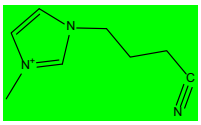	Cl	239.05	228.56	−10.49	224.78	−14.27	225.66	−13.39
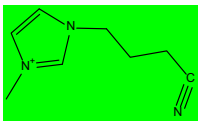	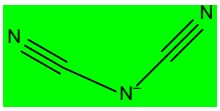	201.35	216.45	15.10	196.03	−5.32	205.38	4.03
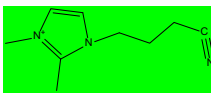	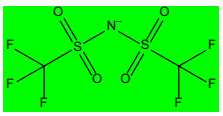	211.65	215.51	3.86	210.01	−1.64	225.04	13.39

Table 1 continued

Cation	Anion	Exp.*	Eq. (2)	Dev	Eq. (3)	Dev	Yan et al.	Dev
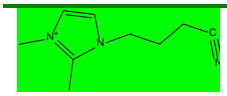	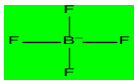	226.65	206.47	−20.18	229.73	3.08	227.17	0.52
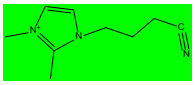	Cl							
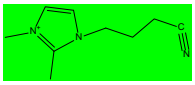	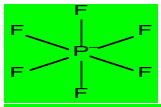	254.25 237.65	225.16 229.59	−29.09 −8.06	248.91 222.59	−5.34 −15.06	240.60 231.87	−13.65 −5.78
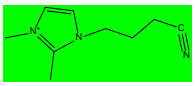	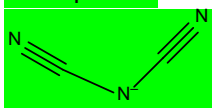	212.15	213.05	0.90	212.61	0.46	221.58	9.43
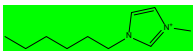	Cl	198.15	206.28	8.13	208.37	10.22	207.09	8.94
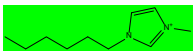	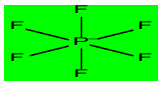	195.15	210.72	15.57	195.02	−0.13	199.66	4.51
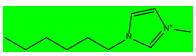	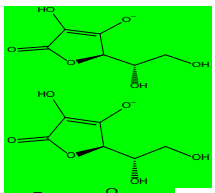	240.82	222.55	−18.27	241.90	1.08	250.62	9.80
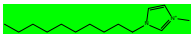		230.81	218.13	−12.68	238.89	8.08	229.51	−1.30
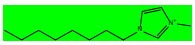	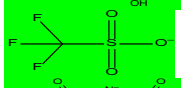	193.15	196.46	3.31	197.14	3.99	200.99	7.84
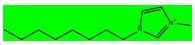	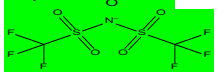	187.15	194.11	6.96	180.73	−6.42	185.38	−1.77
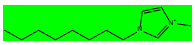	Cl	186.15	203.75	17.60	206.65	20.50	201.13	14.98
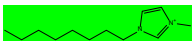	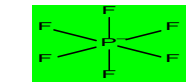	191.15	208.19	17.04	193.31	2.16	198.53	7.38
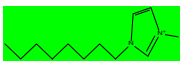		187.15	182.17	−4.98	185.44	−1.71	192.20	5.05
	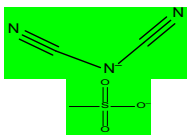	184.15	191.64	7.49	177.90	−6.25	186.73	2.58
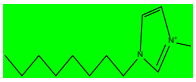		238.21	220.02	−18.19	240.18	1.97	246.49	8.28
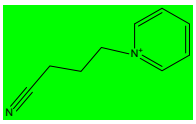	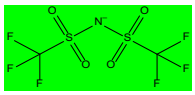	210.85	224.69	13.84	218.21	7.36	217.03	6.18
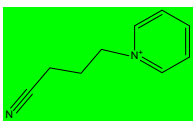	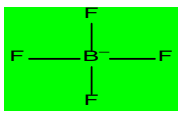	217.15	215.65	−1.50	211.38	−5.77	217.86	0.71

Table 1 continued

Cation	Anion	Exp.*	Eq. (2)	Dev	Eq. (3)	Dev	Yan et al.	Dev
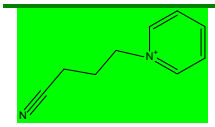	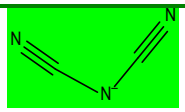	208.85	222.23	13.38	220.81	11.96	212.36	3.51
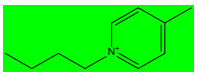	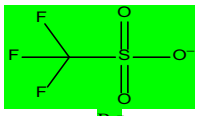	205.15	205.84	0.69	205.31	0.16	203.76	–1.39
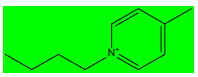	Br$^-$	235.15	230.82	–4.33	230.93	–4.22	232.75	–2.40
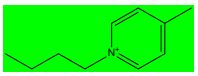	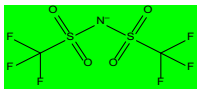	193.15	203.49	10.34	202.47	9.32	193.26	0.11
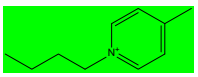	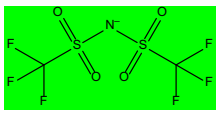	203.00	194.45	–8.55	195.64	–7.36	197.83	–5.17
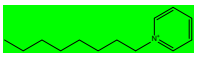	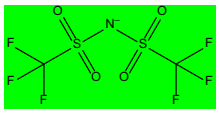	195.15	198.14	2.99	198.45	3.30	196.22	1.07
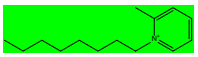	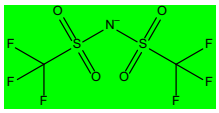	201.15	196.84	–4.31	197.47	–3.68	203.21	2.06
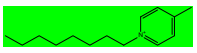	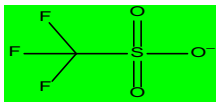	208.15	199.19	–8.96	200.31	–7.84	207.75	–0.40
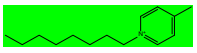	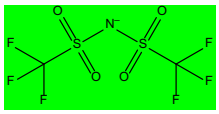	196.15	196.84	0.69	197.47	1.32	192.12	–4.03
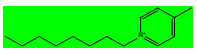	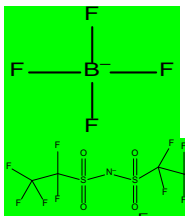	209.15	187.80	–21.35	190.63	–18.52	198.88	–10.27
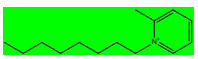		198.15	189.96	–8.19	192.08	–6.07	191.33	–6.82
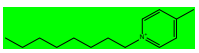	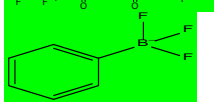	216.15	215.36	–0.79	215.24	–0.91	199.81	–16.34
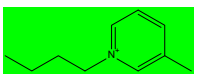	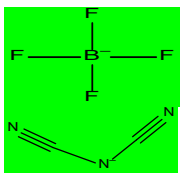	194.00	194.45	0.45	195.64	1.64	203.99	9.99
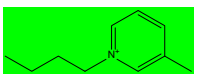		185.00	201.02	16.02	205.07	20.07	198.40	13.40
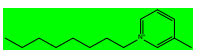	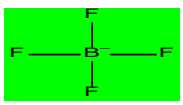	201.00	187.80	–13.20	190.63	–10.37	206.55	5.55

Table 1 continued

Cation	Anion	Exp.*	Eq. (2)	Dev	Eq. (3)	Dev	Yan et al.	Dev
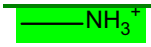	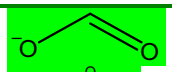	164.95	157.89	−7.06	170.64	5.69	172.54	7.59
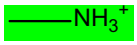	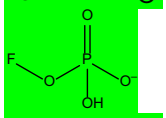	225.35	198.70	−26.65	224.38	−0.97	235.41	10.06
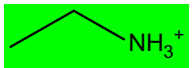	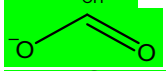	145.65	170.78	25.13	141.96	−3.69	151.02	5.37
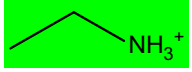	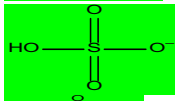	176.75	179.43	2.68	183.74	6.99	185.26	8.51
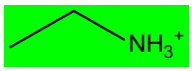	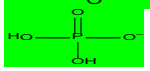	241.85	233.46	−8.39	234.06	−7.79	240.95	−0.90
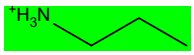	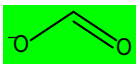	148.45	177.66	29.21	148.39	-0.06	155.19	6.74
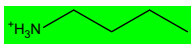	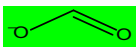	153.05	181.93	28.88	152.38	−0.67	153.64	0.59
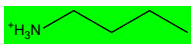	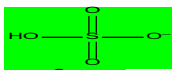	209.75	190.58	−19.17	194.16	−15.59	196.34	−13.41
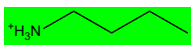	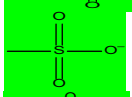	223.15	196.12	−27.03	221.75	−1.40	203.67	−19.48
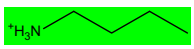	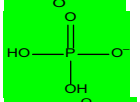	239.85	244.61	4.76	244.48	4.63	247.26	7.41
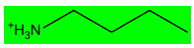	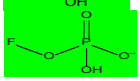	223.05	222.74	−0.31	225.12	2.07	222.48	−0.57
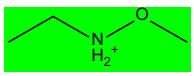	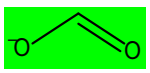	170.15	186.01	15.86	161.44	−8.71	162.69	−7.46
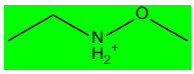	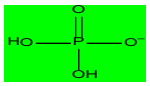	252.85	248.70	−4.15	245.38	−7.47	259.17	6.32
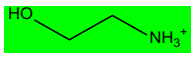	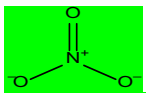	185.75	169.27	−16.48	179.83	−5.92	189.86	4.11
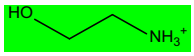	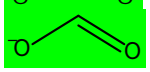	184.85	182.80	-2.05	190.36	5.51	172.07	−12.78
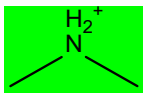	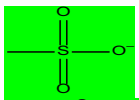	178.15	184.97	6.82	187.19	9.04	197.49	19.34
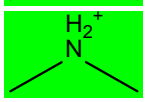	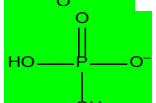	236.35	233.46	−2.89	234.06	−2.29	240.95	4.60
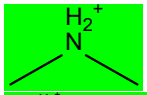	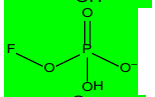	221.65	211.59	−10.06	214.70	−6.95	211.40	−10.25
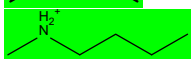	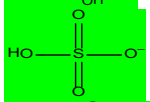	193.55	193.49	−0.06	196.89	3.34	195.52	1.97
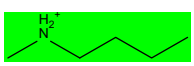	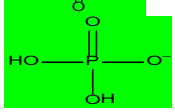	237.15	247.53	10.38	247.20	10.05	244.14	6.99

Table 1 continued

Cation	Anion	Exp.*	Eq. (2)	Dev	Eq. (3)	Dev	Yan et al.	Dev
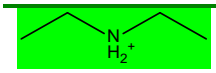	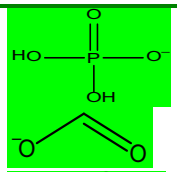	256.45	244.61	−11.84	244.48	−11.97	247.26	−9.19
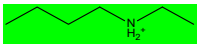		153.55	186.96	33.41	157.08	3.53	146.53	−7.02
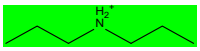	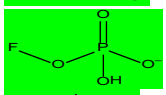	241.65	227.77	−13.88	229.82	−11.83	223.71	−17.94
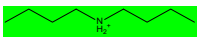		156.75	189.82	33.07	159.76	3.01	150.68	−6.07
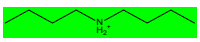	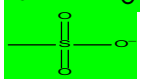	224.15	204.01	−20.14	229.13	4.98	206.64	−17.51
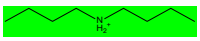	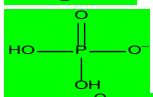	257.55	252.50	−5.05	251.85	−5.70	250.40	−7.15
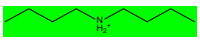		233.65	230.63	−3.02	232.49	−1.16	232.14	−1.51
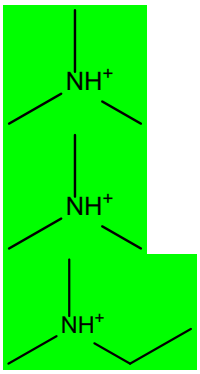	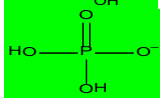	236.45	240.34	3.89	240.48	4.03	244.34	7.89
	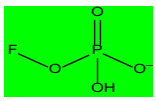	228.65	218.46	−10.19	221.12	−7.53	216.38	−12.27
	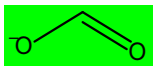	152.05	181.93	29.88	152.38	0.33	152.33	0.28
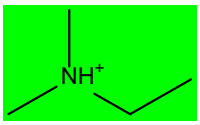	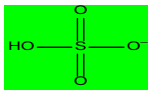	181.75	190.58	8.83	194.16	12.41	193.39	11.64
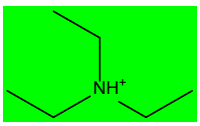	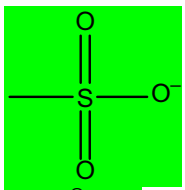	176.65	201.15	24.50	169.73	−6.92	205.29	28.64
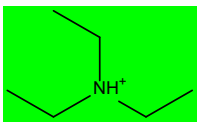		240.95	249.64	8.69	249.18	8.23	248.95	8.00
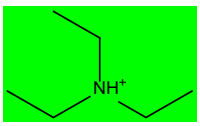	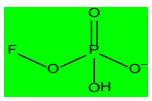	213.45	227.77	14.32	229.82	16.37	227.19	13.74
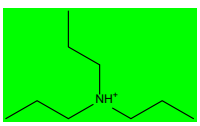	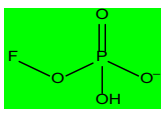	216.55	231.64	15.09	233.44	16.89	224.54	7.99

Table 1 continued

Cation	Anion	Exp.*	Eq. (2)	Dev	Eq. (3)	Dev	Yan et al.	Dev
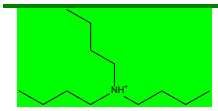	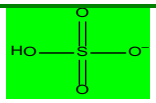	216.05	201.61	−14.44	204.47	−11.58	199.87	−16.18
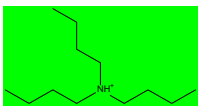	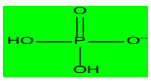	254.35	255.64	1.29	254.79	0.44	242.66	−11.69
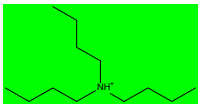	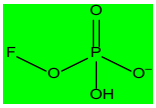	214.05	233.77	19.72	235.43	21.38	226.01	11.96
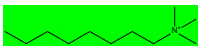	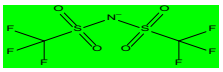	196.15	171.14	−25.01	198.43	2.28	185.25	−10.90
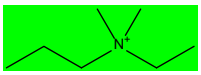	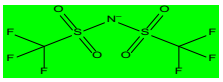	178.15	167.34	−10.81	173.14	−5.01	193.22	15.07
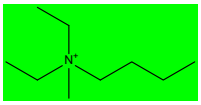	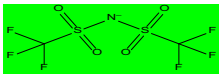	184.15	169.61	−14.54	175.27	−8.88	187.57	3.42
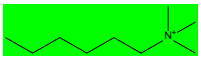	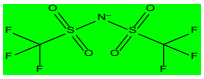	197.15	169.61	−27.54	196.99	−0.16	188.12	−9.03
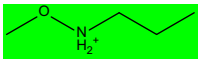	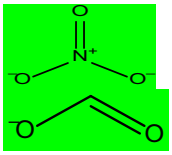	190.45	174.70	−15.75	186.01	−4.44	186.26	−4.19
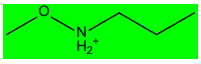		156.75	188.23	31.48	163.96	7.21	155.60	−1.15
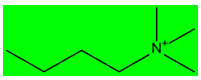	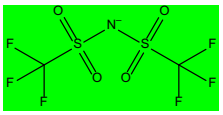	195.15	167.34	−27.81	194.87	−0.28	194.49	−0.66
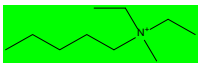	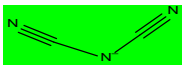	188.15	167.98	−20.17	178.65	−9.50	189.24	1.09
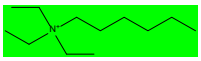	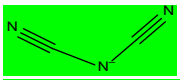	191.15	169.27	−21.88	179.85	−11.30	186.70	−4.45
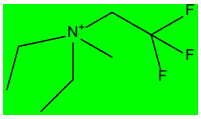	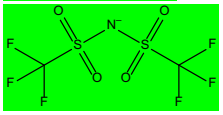	203.15	160.28	−42.87	203.45	0.30	202.32	−0.83
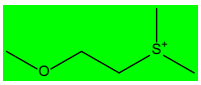	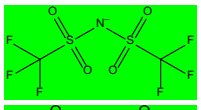	170.15	160.53	−9.62	159.97	−10.18	162.28	−7.87
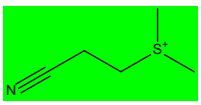	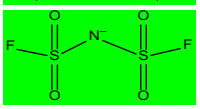	191.15	182.95	−8.20	177.59	−13.56	174.70	−16.45
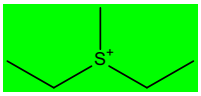	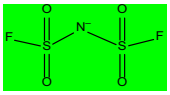	149.15	152.90	3.75	154.25	5.10	148.85	−0.30

Table 1 continued

Cation	Anion	Exp.*	Eq. (2)	Dev	Eq. (3)	Dev	Yan et al.	Dev
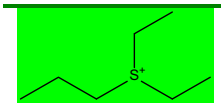	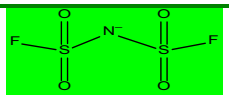	152.15	161.46	9.31	162.92	10.77	160.04	7.89
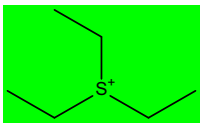	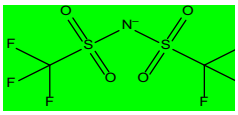	151.15	157.68	6.53	159.09	7.94	156.11	4.96
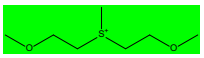	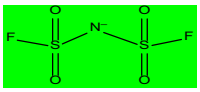	174.15	170.99	–3.16	169.64	–4.51	178.53	4.38
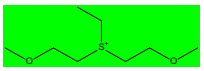	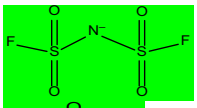	171.15	183.11	11.96	179.84	8.69	179.68	8.53
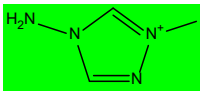	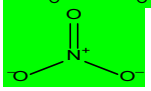	219.15	227.12	7.97	224.79	5.64	212.97	–6.18
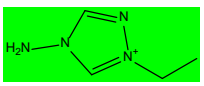	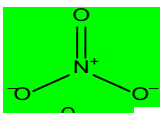	218.15	222.11	3.96	221.68	3.53	219.10	0.95
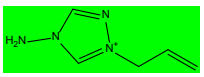	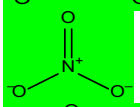	223.15	228.77	5.62	227.63	4.48	225.90	2.75
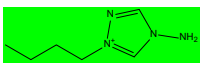	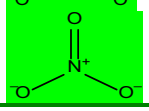	223.15	215.08	–8.07	217.31	–5.84	226.28	3.13

[a] Experimental data were taken from Yan et al. [20]

However, the following re-optimized correlation can be derived using multiple linear regression method [24, 25]:

$$T_{g,IL}^{corr} = 279.95 + \frac{2066.1(n_C)_{cat} - 415.58(n_H)_{cat} + 1981.0(n_N)_{cat} + 1443.8(n_O)_{cat}}{\text{Molar mass}_{cat}} - \frac{1942.9(n_C)_{ani} + 2696.5(n_N)_{ani} + 2579.2(n_O)_{ani} + 4139.5(n_F)_{ani} + 6081.7(n_{Cl})_{ani} + 12420(n_{Br})_{ani} + 4894.0(n_S)_{ani}}{\text{Molar mass}_{ani}} + 24.141T_{IL,g}^{+} - 27.150T_{IL,g}^{-} \quad (3)$$

where $T_{g,IL}^{corr}$ is the corrected glass transition temperature in K; $T_{g,IL}^{+}$ and $T_{g,IL}^{-}$ are two correcting functions that depend on the contribution of some specific cations and anions. The values of $T_{g,IL}^{+}$ and $T_{g,IL}^{-}$ corresponding to specific cations or anions are given in Table 2. For specification of the values of $T_{g,IL}^{+}$ and $T_{g,IL}^{-}$, several steps have been done: (1) The predicted data of Eq. (2) were compared with experimental data and large deviations for various cations and anions were recognized; (2) positive and negative large deviations were identified; (3) specific cations and anions that show large deviations were specified; (4) different relative numbers have been initially selected and regression have been done many times to obtain the least value of the root mean square (rms) deviations of predictions. The

Table 2 Contribution of $T^{+}_{g,IL}$ and $T^{-}_{g,IL}$ in ionic liquids

$T^{+}_{g,IL}$		
Cation	Anion	$T^{+}_{g,IL}$
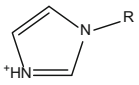	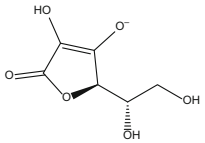	2.0
		0.7
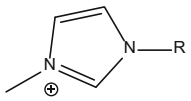 R=alkyl group	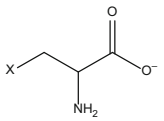	1.1 (if X containing imidazole ring, –SH and 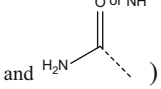)
		2.0 (if X containing 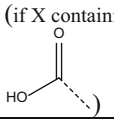)
	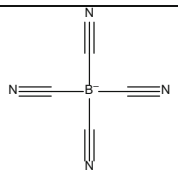	1.1
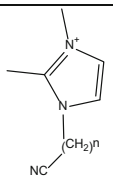	BF_4^-, Cl^-	1.1
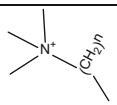	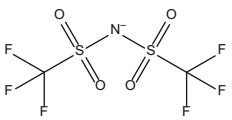	0.9
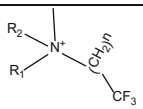		1.8
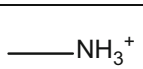	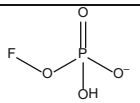	1.0
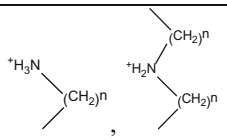	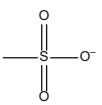	1.0

Table 2 continued

$T_{g,IL}^{-}$		
Cation	Anion	0.5
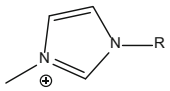	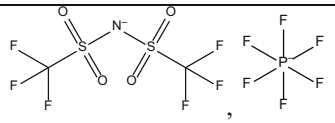	0.7
R=alkyl group, it may contain –CN group	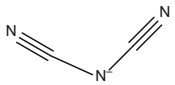	0.5
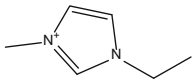	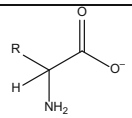	1.5
	R= alkyl group, it may contain sulfur	
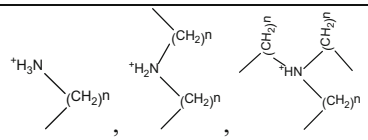	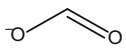	1.2
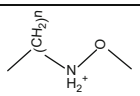		1.0
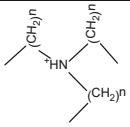	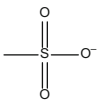	

Table 3 Standardized coefficients and some statistical parameters of Eq. (2)

	Coefficients	Standard error	p value	Lower bound (95%)	Upper bound (95%)
Intercept	322.62	35.00	3.24E−16	253.45	391.80
$(n_C)_{cat}$/Molar $mass_{cat}$	2153.5	395.6	2.18E−07	1371.6	2935.4
$(n_H)_{cat}$/Molar $mass_{cat}$	−554.10	70.30	6.93E−13	−693.00	−415.21
$(n_N)_{cat}$/Molar $mass_{cat}$	2202.4	443.8	1.93E−06	1325.2	3079.6
$(n_O)_{cat}$/Molar $mass_{cat}$	1466.9	722.2	0.044065	39.5	2894.3
$(n_C)_{ani}$/Molar $mass_{ani}$	−2355.7	220.4	5.02E−20	−2791.3	−1920.1
$(n_N)_{ani}$/Molar $mass_{ani}$	−3285.6	286.4	4.43E−22	−3851.7	−2719.5
$(n_O)_{ani}$/Molar $mass_{ani}$	−3253.8	338.9	3.35E−17	−3923.6	−2584.1
$(n_F)_{ani}$/Molar $mass_{ani}$	−4929.4	384.3	1.2E−25	−5689.0	−4169.9
$(n_{Cl})_{ani}$/Molar $mass_{ani}$	−7389.7	660.5	2.45E−21	−8695.2	−6084.2
$(n_{Br})_{ani}$/Molar $mass_{ani}$	−15242	1575	2.19E−17	−18357	−12128
$(n_S)_{ani}$/Molar $mass_{ani}$	−5257.9	518.3	1.32E−18	−6282.4	−4233.4

parameters $T^{+}_{g,IL}$ and $T^{-}_{g,IL}$ are equal to zero if the specified cations or anions in Table 2 are not satisfied.

Results and discussion

Statistical parameters of the new model

The values of the coefficient of determination (R^2) of Eq. (2) and Eq. (3) given in Table 1 are 0.663 and 0.932, respectively [25]. R^2 is a measure of the regression model as whole that can be calculated by:

$$R^2 = 1 - \frac{SS_E}{SS_T} \tag{4}$$

$$SS_T = \sum_i (y_i - \bar{y})^2 \tag{5}$$

$$SS_E = \sum_i (y_i - \hat{y}_i)^2 \tag{6}$$

where SS_E and SS_T are residual (error) and total sum of squares; y_i, $\hat{y}_i$ and $\bar{y}$ are the original data, the modeled and the average values, respectively. If the value of R^2 is close to 1, the predicted values by the model are closer to the actual values. Thus, it can be expected that the reliability of Eq. (3) is higher than Eq. (2). The value of R^2 provides the proportion of the variance (fluctuation) of glass transition temperature that is predictable from the other variables given in Eq. (2) or Eq. (3) because it is such that $0 \leq R^2 \leq 1$. As it is seen in Eqs. (2) and (3), the coefficient of $(n_H)_{cat}$ from cation and the coefficients of all of the variables from anion have negative values, which can provide a suitable pathway for getting lower glass transition temperature in a new designed IL through increasing their values.

Tables 3 and 4 show statistical parameters of Eqs. (2) and (3) corresponding to 11 and 13 variables, respectively. The standard error (SE) of the desired model gives an estimation of the deviation of the predicted values by the model with respect to the experimental data. It is calculated by:

$$SE = \sqrt{\frac{\sum_i (y_i - \hat{y}_i)^2}{N - k}} \tag{7}$$

where N is the number of data points; k is the number of regression coefficients to be determined. The values of SE for variables in Eqs. (2) and (3) show the significance of individual variables in predicting the dependent variable. Thus, if the value of SE of a desired variable is small relative to corresponding coefficient, the variable is significant. The p value shows the probability where a parameter estimated from the measured data should have the value that was determined. If p value of a variable is

Table 4 Standardized coefficients and some statistical parameters of Eq. (3)

	Coefficients	Standard error	p value	Lower bound (95%)	Upper bound (95%)
Intercept	279.95	28.34	7.25E−18	223.93	335.96
$(n_C)_{cat}$/Molar mass$_{cat}$	2066.1	313.9	8.16E−10	1445.7	2686.5
$(n_H)_{cat}$/Molar mass$_{cat}$	−415.58	57.67	3.04E−11	−529.57	−301.59
$(n_N)_{cat}$/Molar mass$_{cat}$	1981.0	354.4	1.12E−07	1280.5	2681.6
$(n_O)_{cat}$/Molar mass$_{cat}$	1443.8	574.3	0.013052	308.5	2579.1
$(n_C)_{ani}$/Molar mass$_{ani}$	−1942.9	190.3	1.01E−18	−2319.0	−1566.7
$(n_N)_{ani}$/Molar mass$_{ani}$	−2696.5	240.6	2.56E−21	−3172.0	−2220.9
$(n_O)_{ani}$/Molar mass$_{ani}$	−2579.2	295.1	5.73E−15	−3162.6	−1995.8
$(n_F)_{ani}$/Molar mass$_{ani}$	−4139.5	327.7	4.91E−25	−4787.3	−3491.7
$(n_{Cl})_{ani}$/Molar mass$_{ani}$)	−6081.7	560.9	2.30E−20	−7190.4	−4973.0
$(n_{Br})_{ani}$/Molar mass$_{ani}$	−12420	1323	1.30E−16	−15035	−9805
$(n_S)_{ani}$/Molar mass$_{ani}$	−4894.0	413.0	5.37E−23	−5710.3	−4077.6
$T^{+}_{g,IL}$	24.141	4.122	3.10E−08	15.994	32.289
$T^{-}_{g,IL}$	−27.150	4.028	3.61E−10	−35.113	−19.188

Table 5 Comparison of the predicted $T_{g,IL}/K$ and $T_{g,IL}^{corr}/K$ for further 30 ionic liquids by Eqs. (2) and (3) with the experimental data

Cation	Anion	Exp.*	Eq. (2)	Dev	Eq. (3)	Dev
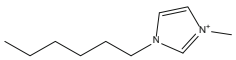	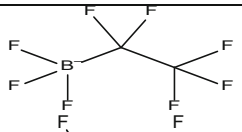	173.15	178.44	5.29	181.87	8.72
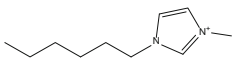	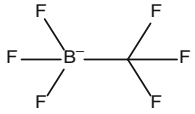	173.15	181.35	8.20	184.19	11.04
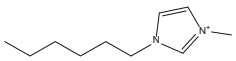	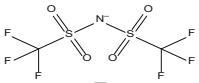	189.00	196.64	7.64	182.45	–6.55
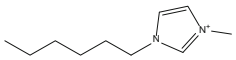	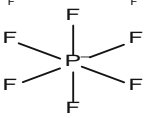	194.00	187.60	–6.40	189.19	–4.81
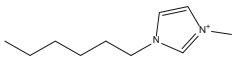	Br^-	224.00	223.97	–0.03	224.48	0.48
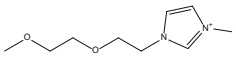	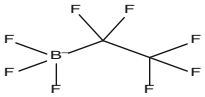	183.15	179.70	–3.45	181.10	–2.05
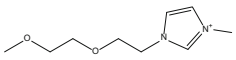	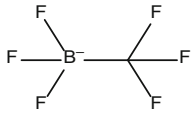	186.15	182.61	–3.54	183.42	–2.73
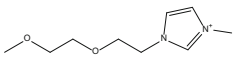	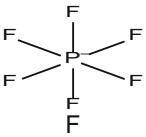	206.30	211.98	5.68	207.82	1.52
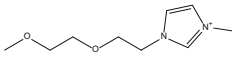	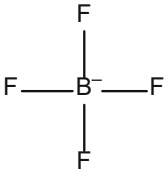	187.15	188.86	1.71	188.41	1.26
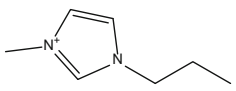	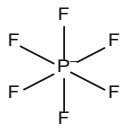	199.15	216.64	17.49	199.04	–0.11
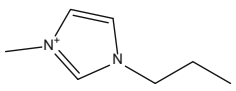	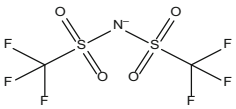	186.15	202.56	16.41	186.47	0.32
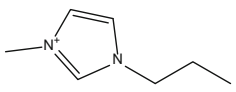	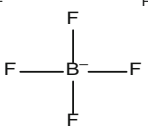	185.15	193.52	8.37	193.20	8.05

Table 5 continued

Cation	Anion	Exp.*	Eq. (2)	Dev	Eq. (3)	Dev
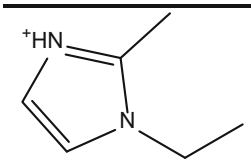	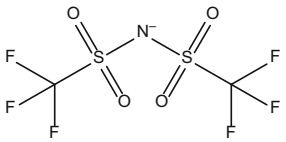	189.15	205.53	16.38	202.06	12.91
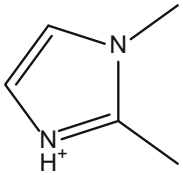	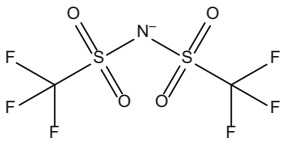	194.15	191.31	–2.84	189.72	–4.43
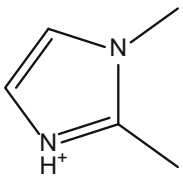	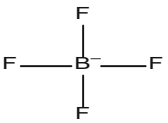	176.15	182.27	6.12	182.88	6.73
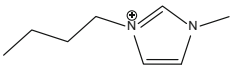	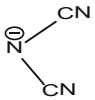	183.15 [26]	200.09	16.94	183.63	0.48
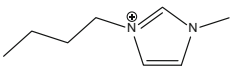	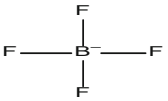	188.15 [26]	191.15	3.00	191.60	3.45
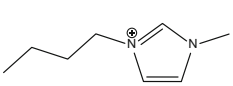	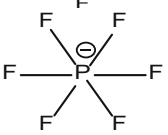	215.15 [26]	212.33	–2.82	209.69	–5.46
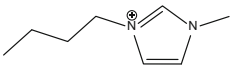	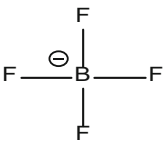	205.15 [26]	189.21	–15.94	190.28	–14.87
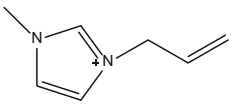		188.15 [27]	210.69	22.54	192.09	3.94
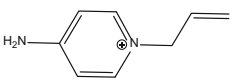		212.15 [28]	216.97	4.82	216.38	4.23
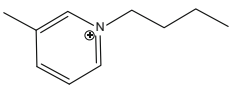	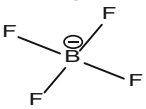	197.15 [29]	194.45	–2.70	195.64	–1.51
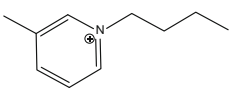	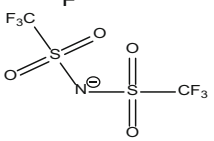	189.15 [29]	203.49	14.34	202.47	13.32
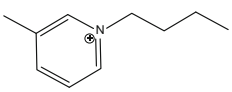	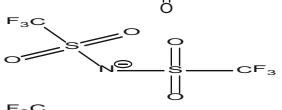	191.15 [29]	199.64	8.49	199.58	8.43
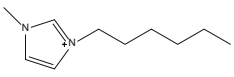	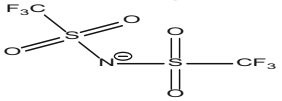	189.15 [29]	196.64	7.49	196.02	6.87

Table 5 continued

Cation	Anion	Exp.*	Eq. (2)	Dev	Eq. (3)	Dev
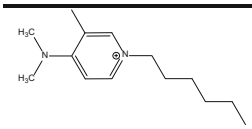	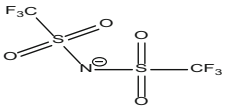	201.15 [29]	217.38	16.23	212.75	11.60
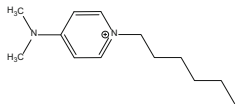	Br$^-$	204.15 [29]	225.35	21.20	226.12	21.97
	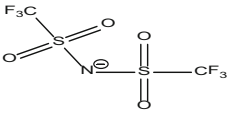	220.15 [29]	198.02	–22.13	197.66	–22.49
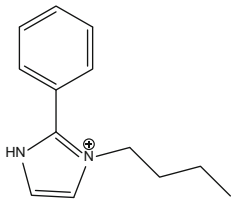	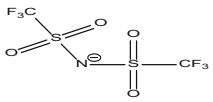	220.15 [30]	218.67	–1.48	214.05	–6.10
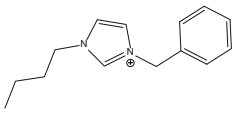	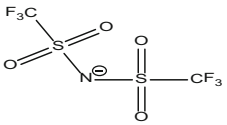	187.15 [30]	216.09	28.94	212.10	24.95

[a] Experimental data were taken from Mousavisafavi et al. [18] except that those are cited

less than 0.05, the effect of the variable will be significant and the observed effect is not due to random variations. Thus, the variables in Eqs. (2) and (3) have a highly significant impact as evidenced by their suitable statistical parameters. As it is indicated in Tables 3 and 4, all of these variables have a highly significant impact as evidenced by their extremely small p values and SEs.

Reliability of the new method

The predicted results of Eqs. (2) and (3) are given in Table 1 and compared with the computer outputs of Yan et al. [20] as one of the best available methods. For 139 data given in Table 1, the rms deviations of predictions for Eq. (2), Eq. (3) and Yan et al. [20] relative to experiment are 16.96, 7.60 and 9.28 K, respectively. However, the reliability of Eq. (3) is surprisingly higher than complex computer outputs of QSPR model of Yan et al. [20].

Table 5 contains glass transition temperature of further 30 ILs, which have been tested for checking the reliability of Eqs. (2) and (3). The rms deviations of the predicted results relative to the measured glass transition temperature for Eqs. (2) and (3) are 12.50 and 9.92 K, respectively, on the basis of data given in Table 5. According to the predicted results in both Tables 1 and 5, Eq. (3) gives more reliable predictions than Eq. (2).

As it is seen in Table 1, maximum deviations are 49.24, 21.38 and 31.81 K for Eq. (2), (3) and Yan et al. [20] relative to experiment, respectively. Maximum errors for Eq. (2) and (3) in Table 5 are also 28.94 and 24.95 K, respectively. By comparing geometrical complexities of different derivatives of imidazolium, pyridinium, ammonium and sulfonium given in Tables 1 and 5, it is found that the overall agreement of the new simple approach with reported glass transition temperature is quite good. As it is indicated in Eq. (3), there are four pathways for maximizing glass transition temperature of ILs: (1) reducing $(n_H)_{cat}$; (2) increasing $(n_C)_{cat}$, $(n_N)_{cat}$ and $(n_O)_{cat}$; (3) decreasing $(n_C)_{ani}$, $(n_N)_{ani}$,$(n_O)_{ani}$, $(n_F)_{ani}$, $(n_{Cl})_{ani}$, $(n_{Br})_{ani}$ and $(n_S)_{ani}$; and (iv) selecting those ILs that have $T^{+}_{g,IL}$. Thus, Eq. (3) provides the easiest pathway for designing IL derivatives containing the desired values of the glass transition temperature.

Conclusions

Two simple correlations have been introduced to predict the glass transition temperature of five kinds of ILs including imidazolium, pyridinium, ammonium, sulfonium and triazolium. In contrast to available QSPR methods, there is no need to use complex descriptors, computer

codes and the expert users. Equation (3) provides more reliable predictions than Yan et al. [20] as one of the best of the predictive methods. Equations (2) and (3) are based on a suitable combination of elemental composition. Moreover, the existence of two correcting functions $T^{+}_{g,IL}$ and $T^{-}_{g,IL}$ in Eq. (3) is important to improve the predictive reliability of Eq. (2). The predicted results for Eq. (3) gave good results as compared to the best available complex QSPR methods.

Acknowledgements We would like to thank the research committee of Malek-ashtar University of Technology (MUT) for supporting this work. We would also like to thank Professor Dr. T. M. Klapotke for providing complementary information.

References

1. Plechkova NV, Seddon KR. Applications of ionic liquids in the chemical industry. Chem Soc Rev. 2008;37(1):123–50.
2. Eftekhari A, Liu Y, Chen P. Different roles of ionic liquids in lithium batteries. J Power Sources. 2016;334:221–39.
3. Klapötke TM. Chemistry of high-energy materials. 3rd ed. Berlin: Walter de Gruyter GmbH; 2015.
4. Zhang Q, Shreeve JNM. Energetic ionic liquids as explosives and propellant fuels: a new journey of ionic liquid chemistry. Chem Rev. 2014;114(20):10527–74.
5. Klapötke TM, Witkowski TG. Covalent and Ionic Insensitive high-explosives. Propellant Explos Pyrotech. 2016;41:470–83.
6. DeLuca LT, Shimada T, Sinditskii VP, Calabro M, Manzara AP. An introduction to energetic materials for propulsion. In: Chemical Rocket Propulsion. Berlin: Springer; 2017. p. 3–59.
7. Xu H, Li H, Wang J. Density prediction of pyridinium, imidazolium, pyrrolidinium, ammonium, and phosphonium-based ionic liquids using an equation of state. Fluid Phase Equilib. 2016;427:406–13.
8. Mjalli FS, Ahmad O. Density of aqueous choline chloride-based ionic liquids analogues. Thermochimica Acta. 2016;64:8–14.
9. Yan F, Shang Q, Xia S, Wang Q, Ma P. Application of topological index in predicting ionic liquids densities by the quantitative structure property relationship method. J Chem Eng Data. 2015;60(3):734–9.
10. Keshavarz MH, Rahimi R, Akbarzadeh AR. Two novel correlations for assessment of crystal density of hazardous ionic molecular energetic materials using their molecular structures. Fluid Phase Equilib. 2015;402:1–8.
11. Keshavarz MH, Pouretedal HR, Saberi E. A simple method for prediction of density of ionic liquids through their molecular structure. J Mol Liq. 2016;216:732–7.
12. Bolbukh Y, Klonos P, Roumpos K, Chatzidogiannaki V, Tertykh V, Pissis P. Glass transition and hydration properties of polyhydroxyethylmethacrylate filled with modified silica nanoparticles. J Therm Anal Calorim. 2016;125(3):1387–98.
13. Righetti MC, Di Lorenzo ML. Rigid amorphous fraction and multiple melting behavior in poly (butylene terephthalate) and isotactic polystyrene. J Therm Anal Calorim. 2016;126(2):521–30.
14. Blanco I, Cicala G, Latteri A, Saccullo G, El-Sabbagh AMM, Ziegmann G. Thermal characterization of a series of lignin-based polypropylene blends. J Therm Anal Calorim. 2017;127:147–53.
15. Keshavarz MH, Esmaeilpour K, Taghizadeh H. A new approach for assessment of glass transition temperature of acrylic and methacrylic polymers from structure of their monomers without using any computer codes. J Therm Anal Calorim. 2016;126(3):1787–96.
16. Greaves TL, Drummond CJ. Protic ionic liquids: properties and applications. Chem Rev. 2008;108(1):206–37.
17. Mirkhani SA, Gharagheizi F, Ilani-Kashkouli P, Farahani N. An accurate model for the prediction of the glass transition temperature of ammonium based ionic liquids: a QSPR approach. Fluid Phase Equilib. 2012;324:50–63.
18. Mousavisafavi SM, Mirkhani SA, Gharagheizi F, Akbari J. A predictive quantitative structure–property relationship for glass transition temperature of 1, 3-dialkyl imidazolium ionic liquids. J Therm Anal Calorim. 2013;111(1):235–46.
19. Mirkhani SA, Gharagheizi F, Ilani-Kashkouli P, Farahani N. Determination of the glass transition temperature of ionic liquids: a molecular approach. Thermochim Acta. 2012;543:88–95.
20. Yan F, Xia S, Wang Q, Shang Q, Ma P. Predicting the glass transition temperature of ionic liquids by the quantitative structure property relationship method using a topological index. Fluid Phase Equilib. 2013;358:166–71.
21. Gharagheizi F, Ilani-Kashkouli P, Mohammadi AH. A group contribution method for estimation of glass transition temperature ionic liquids. Chem Eng Sci. 2012;81:91–105.
22. Lazzús JA. A group contribution method to predict the glass transition temperature of ionic liquids. Thermochim Acta. 2012;528:38–44.
23. Mokadem K, Korichi M, Tumba K. An enhanced group-interaction contribution method for the prediction of glass transition temperature of ionic liquids. Fluid Phase Equilib. 2016;425:259–68.
24. Palm WJ III. Introduction to MATLAB for engineers. 3rd ed. New York: McGraw-Hill; 2011.
25. Palm WJ. Introduction to MATLAB 7 for Engineers. New York: McGraw-Hill; 2005.
26. Fredlake CP, Crosthwaite JM, Hert DG, Aki SN, Brennecke JF. Thermophysical properties of imidazolium-based ionic liquids. J Chem Eng Data. 2004;49(4):954–64.
27. Zhang Y, JNM Shreeve. Dicyanoborate-based ionic liquids as hypergolic fluids. Angew Chem Int Ed. 2011;50(4):935–7.
28. Bhosale VK, Kulkarni PS. Hypergolic behavior of pyridinium salts containing cyanoborohydride and dicyanamide anions with oxidizer RFNA. Propellant Explos Pyrotech. 2016;41:1013–9.
29. Crosthwaite JM, Muldoon MJ, Dixon JK, Anderson JL, Brennecke JF. Phase transition and decomposition temperatures, heat capacities and viscosities of pyridinium ionic liquids. J Chem Thermodyn. 2005;37(6):559–68.
30. Kermanioryani M, Mutalib MIA, Dong Y, Lethesh KC, Ben Ghanem OBO, Kurnia KA, et al. Physicochemical properties of new imidazolium-based ionic liquids containing aromatic group. J Chem Eng Data. 2016;61:2020–6.